Molecular Crystals and Liquid Crystals Science and Technology. Section A. Molecular Crystals and Liquid Crystals

Publication details, including instructions for authors and subscription information:
http://www.tandfonline.com/loi/gmcl19

Effect of Nematic Liquid Crystals on Hysteresis Width Using Nematic-Cholesteric Phase Transition Mode

Yoshikazu Yabe [a] & Dae-Shik Seo [b]

[a] Development Engineering Department, Engineering Division, Fujitsu Kiden Ltd., 1776 Yanokuchi, Inagi-shi, Tokyo, 206, Japan

[b] Department of Electrical and Computer Engineering, College of Engineering, Yonsei University, 134 Shin-chon-dong, Seodaemun-ku, Seoul, 120-749, Korea

Version of record first published: 24 Sep 2006

Mol. Cryst. Liq. Cryst., Vol. 357, pp. 1-10
Reprints available directly from the publisher
Photocopying permitted by license only

Effect of Nematic Liquid Crystals on Hysteresis Width Using Nematic-Cholesteric Phase Transition Mode

YOSHIKAZU YABE[a] and DAE-SHIK SEO[b,*]

[a]*Development Engineering Department, Engineering Division, Fujitsu Kiden Ltd., 1776 Yanokuchi, Inagi-shi, Tokyo 206, Japan and* [b]*Department of Electrical and Computer Engineering, College of Engineering, Yonsei University, 134 Shin-chon-dong, Seodaemun-ku, Seoul 120–749, Korea*

(Received December 16, 1999; Revised May 30, 2000)

The hysteresis width of nematic liquid crystals (NLCs) on a polyimide (PI) surfaces without side chains in nematic-cholesteric phase transition (NCPT) mode was investigated. The generated pretilt angle of ZLI-1132 was almost the same as that of 4-n-pentyl-4′-cyanobiphenyl (5CB) on a PI surface with both sides rubbed. The phase transition time of ZLI-1132 using NCPT mode was similar to that of 5CB on PI surfaces without rubbing-treatment. However, the hysteresis width increased with relation concentration of ZLI-1132 in a ZLI-1132–5CB mixture. The hysteresis width of NCPT mode was not dependent on pretilt angle. Consequently, the large hysteresis width of NCPT mode is attributed to the high elastic constants of the NLCs.

Keywords: Nematic liquid crystals; polyimide; surface alignment; NCPT mode; pretilt angle; hysteresis width

1. INTRODUCTION

The nematic-cholesteric phase transition (NCPT) mode for liquid crystal (LC) is a well known phenomenon, and it has been used in several types of LC display including the light scattering,[1,2] White-Taylor,[3] and bistable memory types.[4–6] The threshold electric field from nematic to cholesteric phase was derived by de Gennes[7] and that of nematic to cholesteric phase was derived by Greubel.[8] The dependence on the elastic constants and the helical pitch of the LC material was dis-

* Author for correspondence E-mail: dsseo@bubble.Yonsei.ac.kr

cussed. Lin-Hendel, using the anisotropic color-absorption properties of the dichroic dye dopant[9,10] reported the influences of electric field induced texture and phase change behaviour of dye-doped, long pitch, cholesteric, LC films as a function of boundary conditions, materials, and LC thickness-to-helical pitch ratio (d/p).

Applications for projection displays using the light scattering effect of the bistable memory effect of the electric field-induced nematic-cholesteric phase transition phenomenon has been reported by some researchers.[11–13] This display needs no polarizers, and therefore a highly luminant image is obtained. The NCPT mode uses the memory effect of the NLC, and theoretically the information content has no limitation. In order to keep this display drive stable, the width of the electro-optical hysteresis is very important. Previously, we reported on the hysteresis behaviour of surface LC alignment using the NCPT mode on PI surface.[14] The effects of NLCs on the hysteresis width in NCPT mode have not yet been reported. The pretilt angle generation of the NLCs on a PI surfaces was demonstrated and discussed by many investigators.[15–26]

In this work, we report on the effects of NLCs on the hysteresis width of the NCPT mode on a PI surfaces without side chains.

2. EXPERIMENTAL

NCPT mode with positive dielectric anisotropy changes state when the applied voltage increased, as shown in Fig. 1. It changes from a cloudy state, the cholesteric phase F, to a transparent state, the nematic phase H. When the voltage is decreased, it transforms from phase H to a metastable transparent state, nematic phase H′, then to phase F. In phase F, the LC in the panel has a helical structure. Because the axis of the helix are parallel to the glass substrates, incident lights is scattered, making phase F cloudy. In phase H, the LC has no helical structure, but instead has a homeotropic structure. Incident light passes through the homeotropic structure, making phase H transparent. In phase H′, the structure of the LC is homeotropic, but in the centre of the layer the LC molecules are assumed to be slightly inclined. Phase H′ is a metastable homeotropic state. The hysteresis effect is thought to be affected by the specific balance between surface anchoring and the thermal properties of the helical structure.

The width of the hysteresis effect is designated the width of hysteresis Δ, as shown in Fig. 1, is defined as the difference between the voltage V_u^{10}, which gives 10 percent transmittance for cholesteric-nematic phase transitions and the voltage V_d^{90}, which gives 90 percent transmittance for nematic-cholesteric phase transitions. The drive voltage, V_d, is set between V_u^{10} and V_d^{90}, as shown in Fig. 1.

NCPT type hysteresis enables the following four-stage addressing scheme. The first stage is initialization for writing. Applying a voltage with magnitude twice the V_d changes all the pixels from state F to state H. The second stage is the writing using selected pixels. The selected pixels are changed to state F by decreasing voltage and then again applying the drive voltage (V_d). The third stage is the writing at non-selected pixels. The non-selected pixels are maintained in state H′ or state H by continuous application of the drive voltage V_d or twice the V_d. The fourth stage is the maintaining the written images. The selected and non-selected pixels are maintained by reapplying the drive voltage.

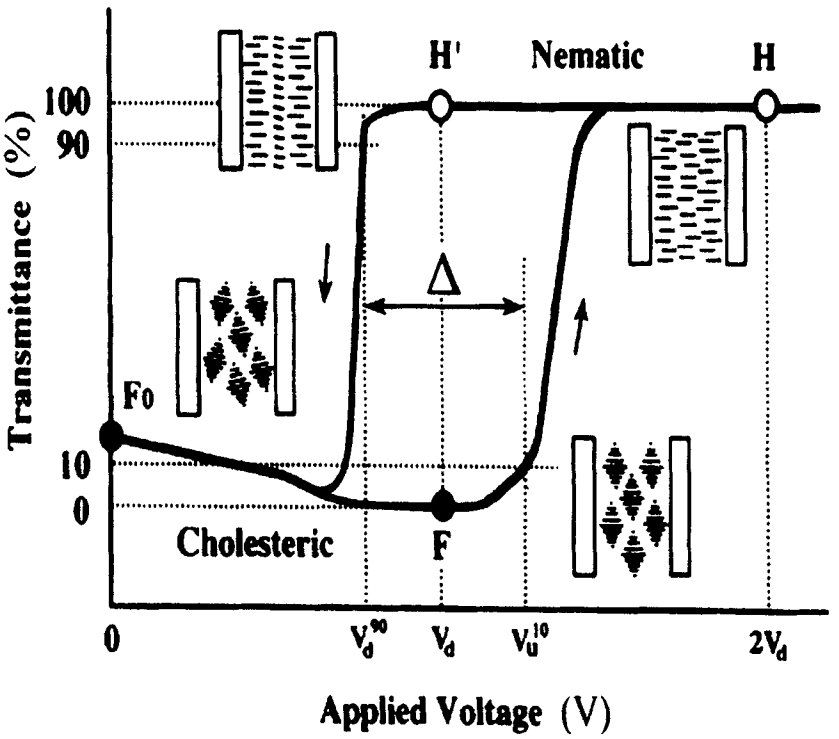

FIGURE 1 Phase transition and transmittance change for the NCPT mode and the definition of hysteresis width Δ

The polymer was used an RN-305 (supplied from Nissan Chemical Industries Co. Ltd.) in this study. The molecular structure of RN-305 has been previously reported.[17] The precursors were coated on ITO coated substrates by spin-coating, and imidized at 250°C for 1 hour. The NCPT-LC layer had a thickness of 5.0 ±

0.1μm, achieved using polymer beads for spacers, and checked by using an LC layer thickness meter made by Otsuka-Electronics Co., Ltd. We used a commercially available mixture for the nematic component (RDP-90613, Rodic Co., Ltd.), as shown in Fig. 2. The helical pitch of the cholesteric phase was 1.0 μ m by using a 9:1 ratio of nematic to chiral nematic LC components. Helical pitches were measured using the Cano method.[27] The relationship between LC thickness and helical pitch was determined by the scattering intensity, and was used a driving voltage of ± 13 V max. General CMOS-LSI, to drive the bistability of the hysteresis effect. Table I shows the physical properties of the used NLCs. Table II shows the used NLC components. We used a rubbing technology that controlled the surface alignment direction of the LC molecules and the rubbing direction was antiparallel for the two substrates. We prepared three kinds of cells-both sides unrubbed, one side rubbed and both sides rubbed.

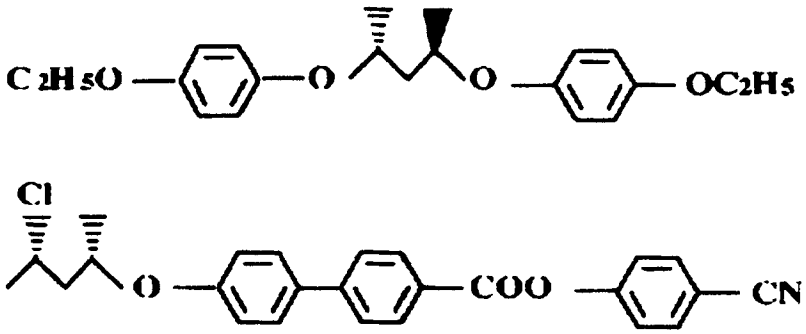

FIGURE 2 Structure of the chiral nematic LCs

TABLE I Physical properties of NLC

NLCs	$K_{11}(\times 10^{-12}N)$	$K_{22}(\times 10^{-12}N)$	$K_{33}(\times 10^{-12}N)$	Δε
5CB	6.2	3.3	8.4	16.1
ZLI-1132	10.1	5.6	19.7	13.1

TABLE II NLC components used (unit : %)

NLCs	*A*	*B*	*C*	*D*	*E*	*F*
5CB	100	80	60	40	20	0
ZLI-1132	0	20	40	60	80	100

Rubbing was done with a rotating cylinder, covered with a fabric consisting of vertical nylon (Yo-15-N, Yoshikawa Chemical Industries Co., Ltd.). The definition of the rubbing strength, RS, was as given in previous papers[15–17] and it is given by

$$\mathrm{RS} = \mathrm{NM}(2\pi \mathrm{rn}/\mathrm{v} - 1), \tag{1}$$

where N is the number of times the rubbing was repeated (usually N=1, in this work), M is the depth of the deformed fibers of the cloth due to the pressed contact (mm), n is the rotational speed of the drum (1000/60 s^{-1}), v is the translating speed of the substrate (7.0mm/s), and r is the radius of the drum. The unit of RS is mm.

In order to measure the pretilt angle, we used the crystal rotation method.[28] The measurements were performed at 20°C. We used the same PI and LC materials, but the LC material was the non-chiral nematic component. Cells were prepared by assembling the substrates antiparallel to the rubbing directions and the rubbing strength was changed. The LC layer thickness was 60 ± 0.3 μm. We changed the thickness relative to that of the cell used for measuring the hysteresis behaviour, in order to measure quickly and correctly the relationship between the rubbing strength and pretilt angle.

Measurement of the hysteresis, as shown in Fig. 1, was carried out using a scheme for driving of the device. The driving schematic, as shown in figure 3, was a special driving method for the NCPT mode, which used the memory effect. Addressing time, t_a, for one pulse width 4ms. Resetting time was t_r for 30 pulses. Holding time was t_h for 2501 pulses of the cholesteric-nematic phase transition and t_r for 2500 pulses of the nematic-cholesteric phase transition. The temperature for measurement of the hysteresis behaviour was 30°C.

3. RESULTS AND DISCUSSION

Figure 4 shows the pretilt angles as a function of NLC components on rubbed PI surfaces without side chains at a strong RS region. It is seen that the pretilt angle of NLC did not vary with the NLC components. The generated pretilt angle of NLCs was about 3.6° on a rubbed PI surface without side chains. We consider that the behaviour of pretilt angle in 5CB was almost the same as seen previous results.[14]

The phase transition time of the NCPT mode as a function of NLC components on a PI surfaces without side chains is shown in Fig. 5. The phase transition time of ZLI-1132 using the NCPT mode on a PI surface was as fast as that of 5CB. It is shown that the phase transition time of the NCPT mode on a PI surface decreases with increasing the ZLI-1132 components.

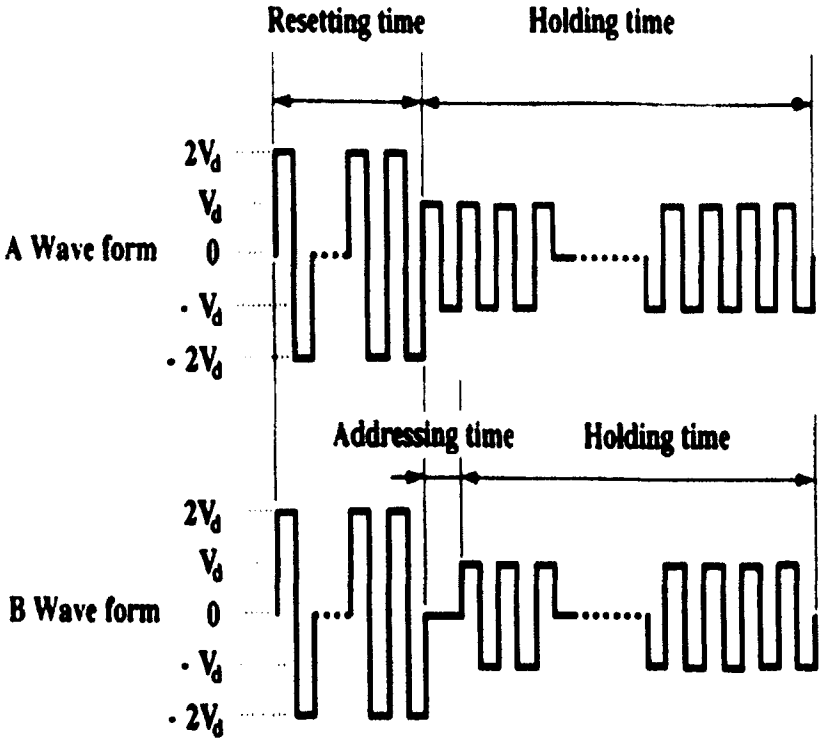

FIGURE 3 Schematic of the driving method. (A)Measured wave form; the phase transition from cholestericto nematic, (B)Measured wave form: the phase transition from nematic to cholesteric

Figure 6 shows the hysteresis width of NCPT mode as a function of NLC components on a PI surfaces without side chains. The hysteresis width of the NCPT mode on a PI surface increases with increasing ZLI-1132 components as shown in Fig. 6 (a), (b), and (c). However, the pretilt angle of NLC did not vary with the increase of the ZLI-1132 components, as shown in Fig. 4. The elastic constants of ZLI-1132 was larger than that of 5CB, as shown in Table I. From these results, we consider that the large hysteresis width for the NCPT mode on a PI surface can be attributed to the high elastic constants of the NLCs. Consequently, the hysteresis width for the NCPT mode depends on the surface alignment of LC molecules and elastic constants of NLCs on a PI surfaces without rubbing-treatment.

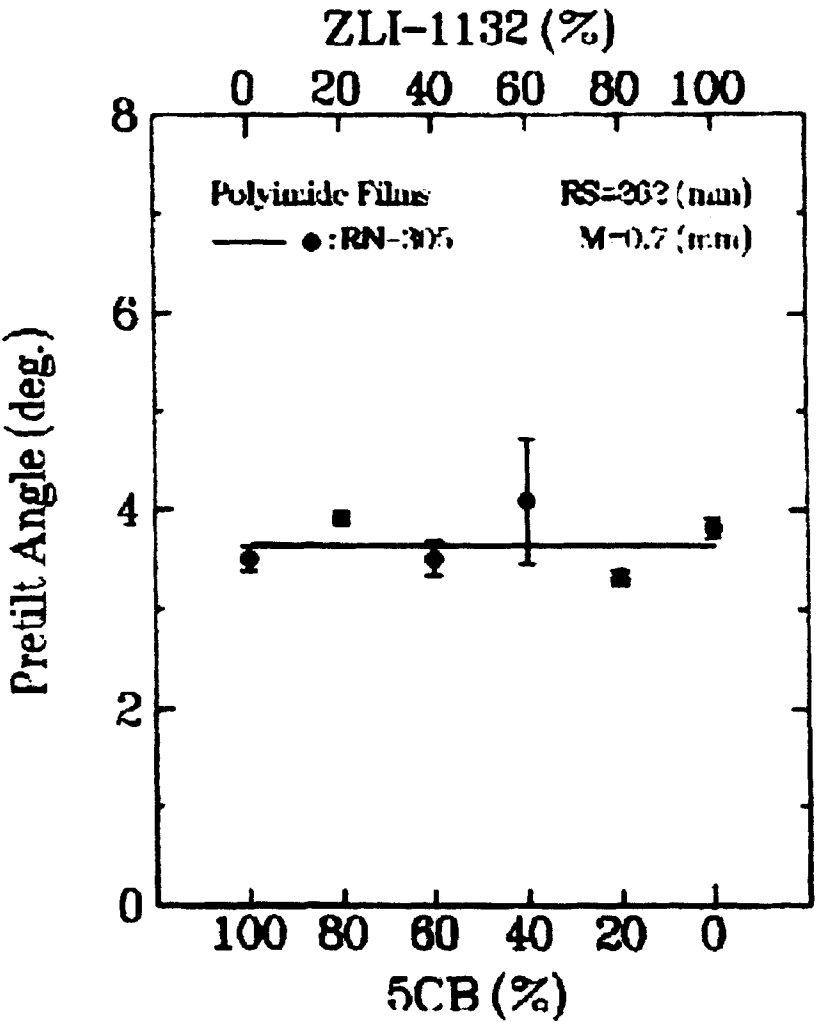

FIGURE 4 Pretilt angles of the NLC as a function of nematic components on a rubbed PI surfaces without side chains

4. CONCLUSION

In conclusion, the effect of hysteresis behaviour of the NCPT mode on a PI surfaces was investigated. The generated pretilt angles of ZLI-1132 was almost the

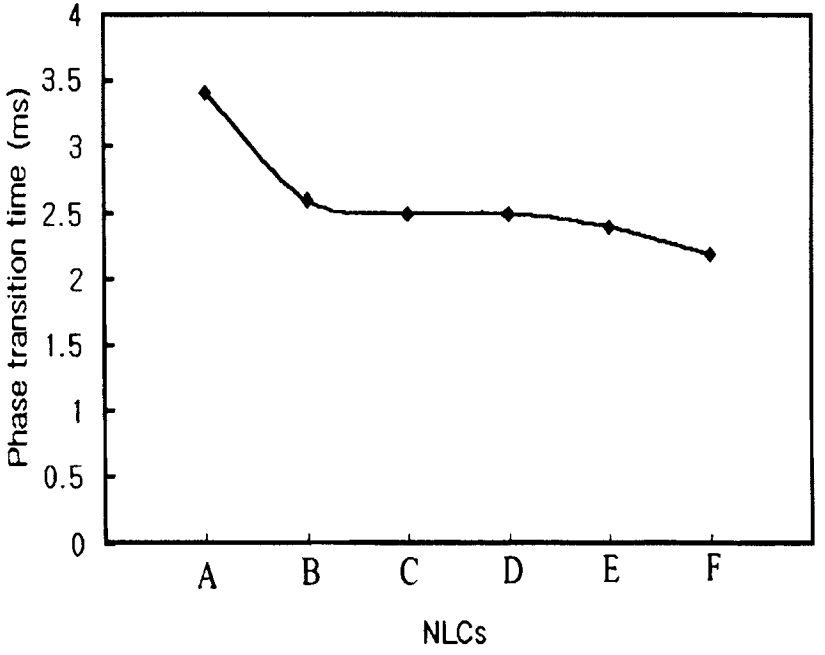

FIGURE 5 Phase transition times of NCPT mode as a function of NLC components on a PI surfaces without side chains

same as those of 5CB on a PI surface with both sides rubbed. The phase transition time of ZLI-1132 using the NCPT mode was similar to that of 5CB on a PI surfaces without rubbing treatment. Also, the hysteresis width of ZLI-1132 using the NCPT mode was larger than that of 5CB. Consequently, the large hysteresis width of the NCPT mode is attributed to the high elastic constants of NLCs.

References

1. J. J. Wysocki, A. Adams and W. Haas, Phys. Rev. Lett. **20**, 1024 (1968).
2. G. H. Heilmeier and J. E. Golgmacher, Appl. Phys. Lett. **13**, 132 (1968).
3. D. L. White and G. N. Taylor, J. Appl. Phys. **45**, 4718 (1974).
4. W. R. Heffner and D. W. Berreman, J. Appl. Phys. **53**, 8599 (1982).
5. K. Kawachi, K. Kato and O. Kogure, Jpn. J. Appl. Phys. **16**, 1673 (1977).
6. K. Kawachi, K. Kato and O. Kogure, Jpn. J. Appl. Phys. **16**, 1263 (1977).
7. P. G. de Gennes, Solid State Communication **6**, 163 (1968).
8. W. Greubel, Appl. Phys. Lett. **25**, 5 (1974).
9. C. G. Lin-Hendel, Appl. Phys. Lett. **38**, 615 (1981).
10. C. G. Lin-Hendel, J. Appl. Phys **53**, 916 (1982).
11. A. Mochizuki, H. Gondo, T. Watanuki, K. Sato, K. Ikegami and H. Okuyama, Pro. SID **26**, 243 (1985).

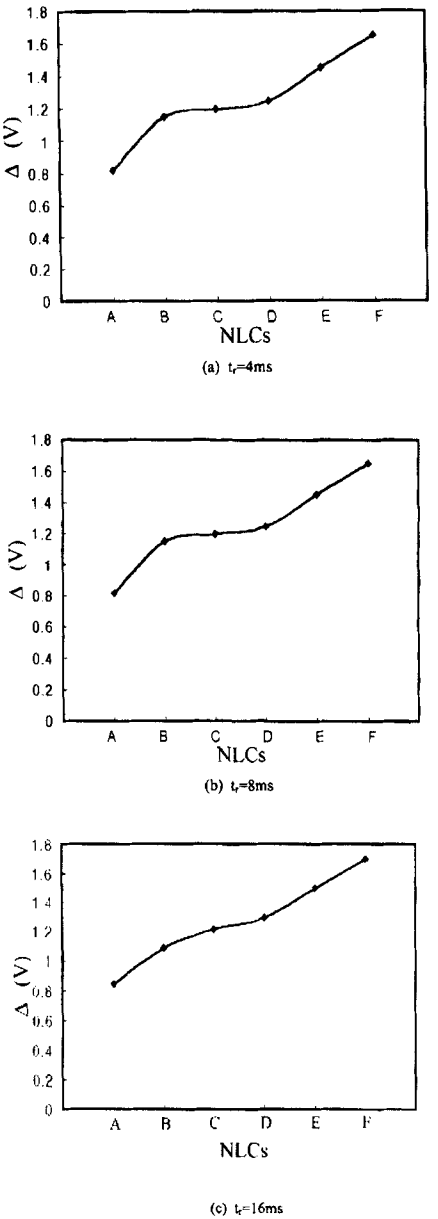

FIGURE 6 Hysteresis width of NCPT mode as a function of NLC components on a PI surfaces without side chains

12. A. Mochizuli, T. Yoshihara, M. Iwasaki, Y. Yamagishi, Y. Koike, M. Haraguchi and Y. Kaneko, Pro. SID **31**, 1888 (1990).
13. Y. Yabe, H. Yamada, T. Hoshi, T. Yoshihara, A. Mochizuki and Y. Yoneda, J. of SID **1**, 43 (1993).
14. Y. Yabe and D.-S. Seo, Liq. Crystals **17**, 847 (1994).
15. D.-S. Seo, K. Muroi and S. Kobayashi, Mol. Cryst. Liq. Cryst. **213**, 223 (1992).
16. D.-S. Seo, S. Kobayashi and M. Nishikawa, Appl. Phys. Lett. **61**, 2392 (1992).
17. D.-S. Seo, K. Araya, N. Yoshida, M. Nishikawa, Y. Yabe and S. Kobayashi, Jpn. J. Appl. Phys. **34**, L503 (1995).
18. J. M. Geary, J. W. Goodby, A. R. Kmetz and J. S. Patel, J. Appl. Phys. **62**, 4100 (1987).
19. H. Fukuro and S. Kobayashi, Mol. Cryst. Liq. Cryst. **163**, 157 (1988).
20. T. Sugiyama, S. Kuniyasu. D.-S. Seo, H. Fukuro and S. Kobayashi, Jpn. J. Appl. Phys. **29**, 2045 (1990).
21. B. O. Myrvold, Y. Iwakabe, S. Oh-hara and K. Kondo, Jpn. J. Appl. Phys. **32**, 5052 (1993).
21. B. O. Myrvold and K. Kondo, Liq. Crystals **17**, 437 (1994).
22. N. A. J. M. Van aerle, Liqu. Crystals **17**, 585 (1994).
23. M. Nishikawa, N. Bessho, T. Natsui, Y. Ohta, N. Yoshida, D.-S. Seo, Y. Iimura and S. Kobayashi, Mol. Cryst. Liq. Cryst. **275**, 15 (1996).
24. M. Nishikawa, T. Miyamoto, S. Kawamura, Y. Tsuda, N. Bessho, D.-S. Seo, Y. Iimura and S. Kobayashi, Mol. Cryst. Liq. Cryst. 258, 285 (1995).
25. D.-S. Seo and S. Kobayashi, Appl. Phys. Lett. **66**, 1202 (1995).
26. D.-S. Seo, S. Kobayashi, M. Nishikawa and Y. Yabe, Liq. Crystals **19**, 289 (1995).
27. R. Cano, Bull. Soc. fr. Miner Cristallogr **91**, 20 (1958).
28. T. J. Scheffer and J. Nehring, J. Appl. Phys. **48**, 1783 (1977).